Dalton Transactions

ROYAL SOCIETY OF CHEMISTRY

PAPER

View Article Online
View Journal | View Issue

Check for updates

Cite this: *Dalton Trans.*, 2022, **51**, 4749

Ligand properties of boryl ligands in bis-boryl rhodium(III) complexes: a case study†

Wiebke Drescher and Christian Kleeberg *

Received 20th December 2021,
Accepted 24th February 2022

DOI: 10.1039/d1dt04276a

rsc.li/dalton

The oxidative addition of five diborane(4) derivatives, symmetrical and unsymmetrical, to $[Rh(PMe_3)_3Cl]$ was studied. Only for the more electron poor diboron derivatives, B_2cat_2, B_2pin_2 and catB–Bpin the resulting octahedral bis-boryl complexes $[(PMe_3)_3Rh(boryl)_2Cl]$ were obtained, while for the more electron rich congeners only the equilibrium oxidative addition (catB–Bdmab) or no significant reaction (pinB–Bdmab) was observed (pin = $(OCMe_2)_2$, cat = 1,2-$O_2C_6H_4$, dmab = 1,2-$(NMe)_2C_6H_4$). By abstraction of the chlorido ligand with NaBArF (BArF = tetrakis-[3,5-bis-(trifluormethyl)-phenyl]-borat) in the presence of a neutral ligand (L = PMe_3, MeCN, MeNC) the corresponding cationic octahedral complexes $[(PMe_3)_3Rh(boryl)_2L]^+$ were obtained. All isolated complexes were fully characterised including single crystal X-ray diffraction and heteronuclear, temperature dependent NMR spectroscopy. Whilst the complexes $[(PMe_3)_3Rh(boryl)_2Cl]$ and $[(PMe_3)_3Rh(boryl)_2L]^+$ show many similarities, their detailed structural and spectroscopic properties depend crucially on the properties of both boryl ligands.

Introduction

Boryl complexes derived from diborane(4) derivatives, in particular B_2cat_2 (**1a**) and B_2pin_2 (**1b**) (pin = $(OCMe_2)_2$, cat = 1,2-$O_2C_6H_4$), are central as reactive intermediates for an ever growing number of transition metal catalysed borylation reactions.[2] Despite their broad application, the relevant boryl complexes are still the subject of ongoing studies.

Theoretically it is well established that the substitution pattern of a boron moiety influences both its properties as a ligand in transition metal complexes as well as the reactivity of the corresponding diborane(4) derivatives.[3] However, experimental studies of series of analogous boryl complexes with distinct boryl ligands are scarce.[3a]

For such a study we rationalized that bis-boryl complexes accessible by oxidative addition of a diborane(4) to low-valent transition metal complexes should be suitable. In particular, when using unsymmetrical diborane(4) derivatives, unsymmetrical bis-boryl complexes result that allow the direct comparison of two distinct boryl ligands within one complex. Platinum (II) bis-boryl complexes of the type $[(Ph_3P)_2Pt((boryl)_2]$ appear suitable complexes, however, we have shown that the boryl ligands in these complexes are not independent,[4] as is – and possibly more pronounced – the case for bis /tris-boryl complexes of cobalt or iridium.[5,6] On the synthetic side, however, the oxidative addition of diboranes(4) to rhodium(I) complexes is reported for different aryloxy as well as alkyloxy based diboranes(4) (Fig. 1).

Given the plethora of reported – though, not necessarily structurally characterized – rhodium(III) bis-boryl complexes we endeavoured to employ the oxidative addition of diboranes (4) to a rhodium(I) complex to access a series of analogous bis-boryl complexes. In particular the report by Marder, Norman and co-worker on the reaction of $[RhCl(PR_3)_3]$ with **1a** to give **2b**, inspired us to use the sterically non-demanding and electron-rich complex $[RhCl(PMe_3)_3]$ for further studies.[1d] Moreover, it could be envisaged that the complexes $[(PMe_3)_3RhCl(boryl)_2]$ resulting from an oxidative addition of a diborane(4) can be converted to the cations $[Rh(PMe_3)_4(boryl)_2]^+$ upon reaction with PMe_3 in the presence of a

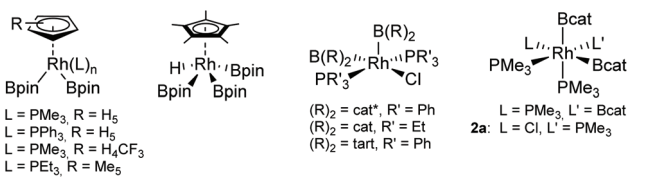

Fig. 1 Examples of rhodium bis- and tris-boryl complexes accessible from diboranes(4) (cat* derivatives = 1,2-O_2-4-*t*BuC_6H_3, 1,2-O_2-3,5-*t*Bu$_2C_6H_2$, 1,2-O_2-3-MeC_6H_3, 1,2-O_2-4-MeC_6H_3, 1,2-O_2-3-MeOC_6H_3, 1,2-$S_2C_6H_4$; tart = *R,R*-(OCH(CO_2Me))$_2$).[1]

Institut für Anorganische und Analytische Chemie, Technische Universität Braunschweig, Hagenring 30, 38106 Braunschweig, Germany.
E-mail: ch.kleeberg@tu-braunschweig.de

† Electronic supplementary information (ESI) available: Additional NMR spectroscopic and crystallographic data. CCDC 2129858–2129867, 2129870 and 2129871. For ESI and crystallographic data in CIF or other electronic format see DOI: 10.1039/d1dt04276a

salt of a weakly coordinating anion. Both classes of complexes should provide ample structural as well as NMR-spectroscopic probes to characterize the donor properties of the boryl ligands.

Results and discussion

In situ NMR study on the reaction of [Rh(PMe$_3$)$_3$Cl] with diboranes(4): [(PMe$_3$)$_3$Rh(boryl)$_2$Cl]

For an initial assessment of the scope of the formation of bis-boryl complexes by reaction of [Rh(PMe$_3$)$_3$Cl] with different diboranes(4) (Scheme 1) an *in situ* NMR study was conducted with a series of five diborane(4) derivatives: the symmetrical diboranes(4) B_2cat_2 (**1a**) and B_2pin_2 (**1b**) as well as the unsymmetrical congeners catB–Bpin[7] (**1c**), catB–Bdmab[7] (**1d**) and pinB–Bdmab[4a] (**1e**) (dmab = 1,2-(NMe)$_2$C$_6$H$_4$).

Following the reactions by *in situ* ^{31}P and ^{11}B NMR spectroscopy the progress of the reaction is indicated by a decrease of the ^{11}B NMR signal (or signals in the case of the unsymmetrical **1c–e**) of the diboranes at, typically, below 38 ppm and the appearance of one or two signals above that, indicative for boryl complexes (Fig. 2).

The ^{11}B NMR data indicate that for **1a** and **1c** the diborane (4) is consumed rapidly, whereas for **1b** a slower reaction is observed. The ^{31}P NMR data give a fitting picture: for **1a–c** after full conversion two signals are found, one doublet in the −10–0 ppm range and second one, a singlet, around −30 ppm. As expected for the formation of [(Me$_3$P)$_3$RhCl(boryl)$_2$] complexes. Both signals are however significantly broadened, as compared *e.g.* to the signals of the starting material [Rh(PMe$_3$)$_3$Cl] (Fig. 2), but also significantly shifted, indicating the formation of new complexes. The broad line shape of the ^{31}P NMR signals is partly due to the quadrupolar nature of the ^{11}B/^{10}B nuclei in the resulting boryl complexes, but also due to the dynamics present (*vide infra*). This is particular apparent in the reaction of **1b** after 0.5 h, while unreacted **1b** is present: the ^{31}P NMR spectrum exhibit only two signals with chemical shifts between those for [Rh(PMe$_3$)$_3$Cl] and **2b**, indicative for rabid exchange (*vide infra*).

The observations are different for the unsymmetrical diamino dialkoxy diboranes(4) **1d** and **1e**. Whilst for **1d** the *in situ* NMR data indicate, according to the characteristic ^{11}B NMR chemical shift of just above 38 ppm, the formation of a boryl complex, in the ^{31}P NMR spectrum only one very broad signal is unambiguously identified, presumably due to rapid exchange between a putative boryl complex and [Rh(PMe$_3$)$_3$Cl]. Whereas for **1e** no consumption of the diborane(4) is evident, however, a broadening of the ^{31}P NMR signals of [Rh(PMe$_3$)$_3$Cl] is stated.

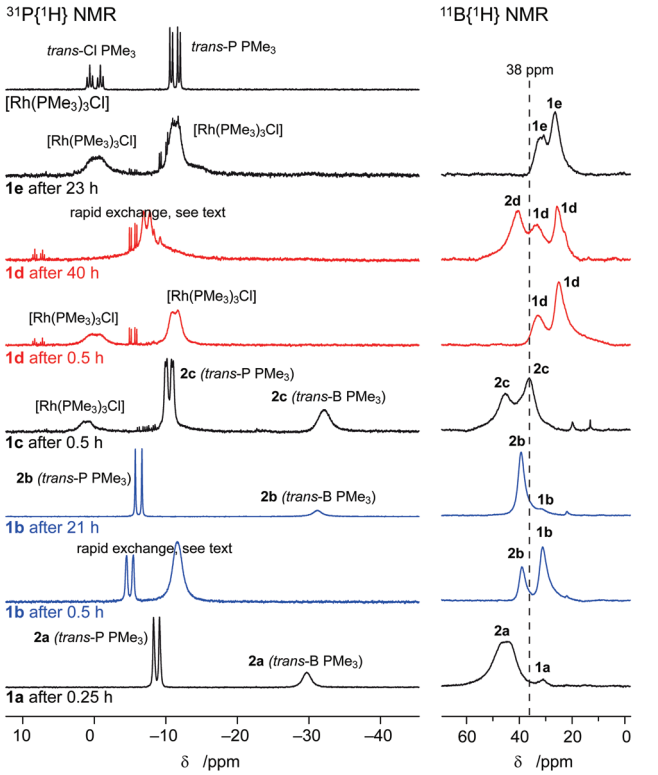

Fig. 2 *In situ* ^{31}P{^{1}H} and ^{11}B{^{1}H} NMR spectra of the reactions of [Rh(PMe$_3$)$_3$Cl] with the diboranes(4) **1a–e** (121.5/96.3 MHz, rt); unassigned signals: unidentified species.[8]

This is well rationalized by the electronic properties of the diboranes(4) **1a–e**. The electron poor B_2cat_2 (**1a**) is more prone to undergo oxidative addition to a metal than the comparably electron rich B_2pin_2 (**1b**), while the unsymmetrical tetraalkoxydiborane catB–Bpin (**1c**) exhibits an intermediate reactivity.

The unsymmetrical diamino dialkoxy diboranes(4), with their very electron rich diamino boron moiety, react more sluggishly (catB–Bdmab (**1d**)) if at all (pinB–Bdmab (**1e**)) (Fig. 2).[8] This observation is in agreement with the general trend that the electron poor B_2cat_2 (**1a**) is more reactive in oxidative addition reactions than the more electron rich B_2pin_2 (**1b**) and diamino diborane(4) derivatives.[1,2,9]

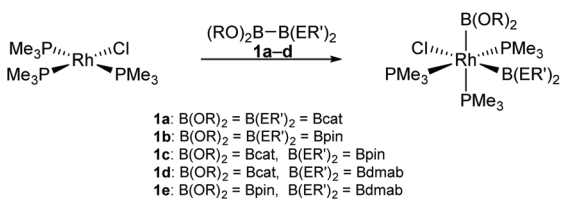

Scheme 1 Envisaged formation of rhodium(III) bis-boryl complexes by oxidative addition of diboranes(4) **1a–d** as studied by NMR spectroscopy.

Isolation of [(PMe$_3$)$_3$Rh(boryl)$_2$Cl] (2a–c)

Based on the results of the *in situ* NMR experiments the isolation of bis-boryl complexes derived from **1a–d** and [Rh(PMe$_3$)$_3$Cl] was explored, whilst the apparently much less reactive **1e** was not included in further studies.

For **1a** and **1c** the bis-boryl tris-phosphine complexes [(Me$_3$P)$_3$RhCl(Bcat)$_2$] (**2a**) and [(Me$_3$P)$_3$RhCl(Bcat)(Bcat)] (**2c**)

start to crystallise as colourless crystalline solids within minutes after combination of the solution of the starting materials (in THF/PhMe and pure PhMe, respectively) and were obtained in excellent 92% and 91% yield, respectively (Scheme 2).

For **1b**, however, the tris-phosphine complexes $[(Me_3P)_3RhCl(Bpin)_2]$ (**2b**) does not crystallise from the reaction mixture. However, upon removal of the solvent *in vacuo*, extractive work-up and crystallization from *n*-pentane mixtures of **3b** and **2b** (**2b·3b**$_n$, up to 71% yield based on Rh) were obtained. Whereas extensive exposure to vacuum during the work-up led to the exclusive isolation of the bis-boryl bis-phosphine complex $[(Me_3P)_2RhCl(Bpin)_2]$ (**3b**) (51% yield). However, **3b** is readily converted to **2b** by addition of a stoichiometric amount of PMe_3. An excess of PMe_3, however, facilitates, in agreement with earlier results on **2a**, the decomposition of **2b**/**3b** leading to the crystallisation of $[Rh(PMe_3)_4]Cl$ and **1b**.[1d]

For the diborane **1d**, already reacting sluggishly in the *in situ* NMR study, only $[(Me_3P)_4RhH(Cl)][B(1,2\text{-}O_2C_6H_4)_2]$ and B_2dmab_2, possible decomposition products of an intermediate rhodium boryl complex, were obtained.[8,10]

It should be emphasised that this formation of the symmetrical diborane B_2dmab_2 from the unsymmetrical **1d** is the only instance were scrambling of unsymmetrical diboranes(4) was observed. In particular was no evidence found for any scrambling of the distinct boryl ligand in **2c**, putatively resulting either in the formation of symmetrical bis-boryl complexes or symmetrical diboranes(4).

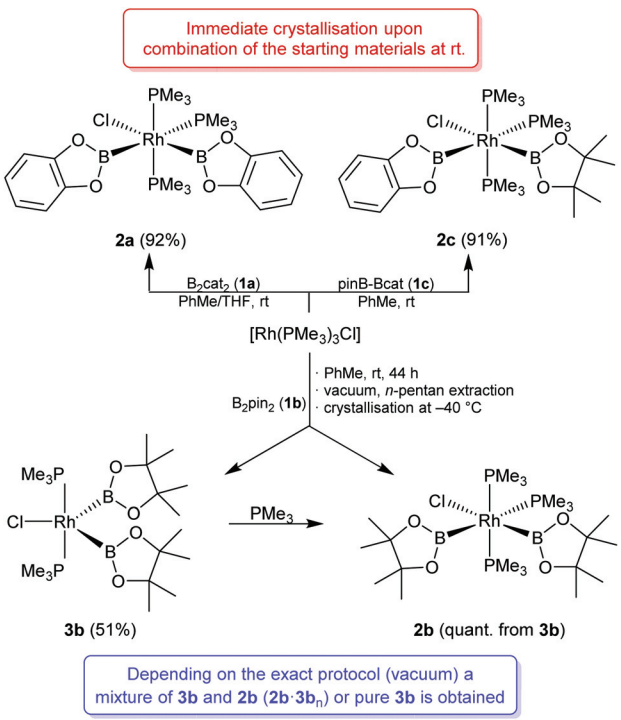

Scheme 2 Synthesis of **2a–c**, **3b** and **2b·3b**$_n$.

Synthesis of cationic rhodium(III) bis-boryl complexes $[(PMe_3)_3Rh(L)(boryl)_2][BArF]$

Whilst the series of boryl complexes **2a–c** allows for a comparison of the boryl ligand donor properties amongst the three different complexes, a comparison of different boryl ligands within a single complex would be interesting. Replacing the chlorido ligand in **2a–c** by an additional PMe_3 ligand leads to the cationic complexes **4a–c** (Scheme 3). These complexes, are straight-forwardly obtained upon reaction of **2a–c** with an equimolar amount of PMe_3 in the presence of Na[BArF] (BArF = *tetrakis*-[3,5-bis-(trifluoromethyl)phenyl]borate). Complex **4c** allows now for a comparison of two different boryl ligands within a single complex.

The replacement of the chlorido ligand in **2c** by other neutral ligands was, in our hands, limited to MeCN and MeNC leading to the well-defined complexes $[Rh(PMe_3)_3(Bcat)(Bpin)(MeCN)][BArF]$ (**5c**) and $[Rh(PMe_3)_3(Bcat)(Bpin)(MeNC)][BArF]$ (**6c**).[8] Attempts to use other ligands such as CO, PEt_3 or $P(OMe)_3$ furnished in our hands $[(Me_3P)_3Rh(CO)_2][BArF]$ or $[(Me_3P)_4Rh][BArF]$ as the only crystallographically identified species.

Structural characterisation: $[(PMe_3)_3Rh(boryl)_2Cl]$

Single crystals of sufficient quality for X-ray diffraction studies were obtained from **2a–c**. Whereas, **2a** crystallises in the monoclinic space-group type $P2_1/n$ with one molecule in the asymmetric unit, **2b** and **2c** were obtained as the solvates **2b**(PhMe) and **2c**$(THF)_{1/2}$, respectively, the first in the monoclinic system in $C2/c$ (Z = 8, Z' = 1), the latter in an orthorhombic space-group *Pbcn* (Z = 8, Z' = 1). In addition a molecular structure of **2b** was also obtained from **2b** co-crystallised with **3b** (**2b·3b**), however, the geometrical molecular data of **2b** differ not significantly and only the data from **2b** are discussed.[8]

None of the complexes **2a–c** exhibits crystallographic point symmetry in the solid state and share the same general structural motifs. However, subtle changes indicate the different ligand properties of the Bpin and Bcat ligands.

The complexes **2a–c** exhibit six-fold coordinated rhodium atoms (Fig. 3) in a distorted octahedral geometry with the apical positions occupied by two PMe_3 ligands, whereas the equatorial plane is occupied by two *cis* boryl ligands, one additional PMe_3 ligand and the chlorido ligand. This geometry in the solid state resembles the geometry in solution, as indicated by NMR data (*vide supra*).

The *cis* arrangement of the two boryl ligands in **2a–c** is evidence for their strong σ-donor properties and, hence, *trans*

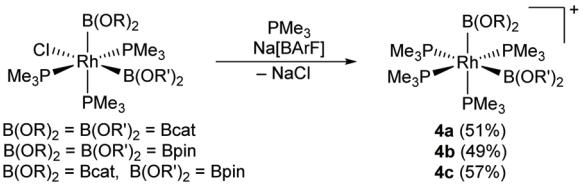

Scheme 3 Synthesis of the cationic complex $[(PMe_3)_4Rh(boryl)_2][BArF]$.

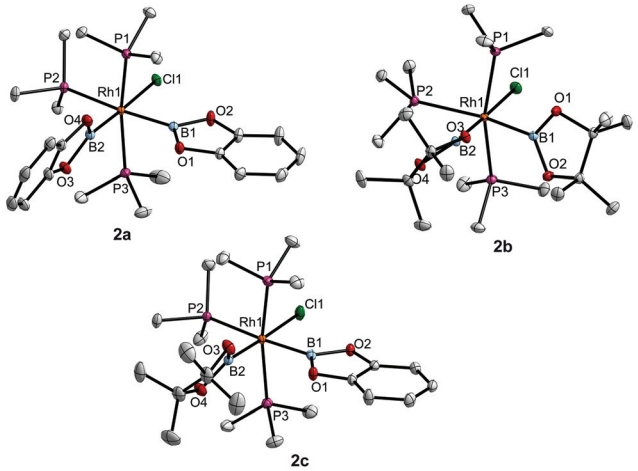

Fig. 3 Molecular structures of **2a–c** from X-ray diffraction studies on **2a**, **2b**(PhMe) and **2c**$(THF)_{1/2}$.[H]

influence of the boryl ligand disfavouring a mutual *trans* arrangement. In fact, only two complexes with *trans* boryl ligands are known so far, both exhibiting either geometric or electronic peculiarities.[5a,12]

The ligand properties of the boryl ligands, in particular the *trans* influence is further crucial for the complex geometry (Table 1). The *trans*-B P–Rh distances (P2–Rh1) are by 0.09–0.14 Å longer as the, within **2a–c** quite consistent, *trans*-P P–Rh distances (P1–Rh1 and P3–Rh1) of 2.32 Å. Moreover, in **2c** the chlorido ligand, as weaker σ-donor ligand than PMe_3, occupies the position *trans* to the more *trans* influencing ligand Bpin.[3] *Vice versa*, the B–Rh distances *trans* to a PMe_3 ligand (B1–Rh1) are longer than those of the same boryl ligand *trans* to the chlorido ligand.

The B···B distance (in correlation with the B1–Rh1–B2 angle) is by more than 0.3 Å shorter for the bis-Bpin complex **2b** than for the bis-Bcat complex **2a**, whereas in the unsymmetrical Bpin/Bcat complex **2c** an only slightly smaller value as in **2a** is observed. The B···B distances in **2a–c** are significantly longer than in diboranes(4) (1.7 Å), but also than in cobalt and iridium bis /tris-boryl complexes were B···B interactions have been evidenced by computational means (*mer*-$[(Me_3P)_3Co(Bcat)_3]$ (2.1541(5) Å), $[(R_3P)_3Co(Bcat)_2]$ (2.185–2.271 Å) and $[((C_6H_4)(NPh)(NCH_2PPh_2)B)_2IrCl]$ (2.221 Å)).[5–7,13] However, the B···B distance in **2b** is in the range also found for a series of platinum complexes $[(Ph_3P)_2Pt(boryl)_2]$ (2.44–2.56 Å) where we proposed a certain amount of B···B interaction.[4]

Structural characterisation: $[(PMe_3)_4Rh(boryl)_2]^+$

The cationic complexes **4a–c** crystallise with one formula unit in the asymmetric unit as **4b** ($P2_1/n$) or as the solvates **4a** (PhMe) ($P\bar{1}$) and **4c**(THF) ($P2_1/n$), respectively. The complex cations are situated on general positions not exhibiting any higher point symmetry.

Structurally, the complex cations resemble the parent chlorido complexes **2a–c** (Table 1, Fig. 4), with the chlorido ligand exchanged for an additional PMe_3 ligand.

These complexes allow now a direct comparison of the geometries of the two *trans*-B–Rh–P entities under virtually identical conditions. The B–Rh distances are slightly shorter for the bis-Bcat complex **4a** than for the complexes **4b** and **4c**. In the unsymmetrical complex **4c** both B–Rh distances are identical within error and rather on the long side, in between the distance found for **4a** and **4b**. This suggests that the B–Rh distances are not very characteristic for a certain boryl ligand.[4]

A look on the P–Rh distances reveals that, as for **2a–c**, the *trans*-B P–Rh distances are by about 0.1 Å larger than the *trans*-P P–Rh distances (*vide supra*). The *trans*-B P–Rh distances

Table 1 Selected geometrical data of the molecular structures of the 6-coordinate rhodium boryl complexes of **2a–c** and the complex cations in **4a–c**

	2a	**2b** from **2b** (PhMe)	**2c** from **2c** $(THF)_{1/2}$	**4a** from **4a** (PhMe)	**4b**	**4c** from **4c** (THF)
Rh1–Cl [Å]	2.5315(3)	2.5539(2)	2.5686(7)			
Rh1–P1 [Å]	2.3176(3)	2.3213(2)	2.3164(7)	2.3349(8)	2.3534(8)	2.3481(5)
Rh1–P2 [Å]	2.4171(3)	2.4660(2)	2.4241(6)	2.4524(8)	2.4325(8)	2.4694(5)
Rh1–P3 [Å]	2.3271(3)	2.3270(2)	2.3261(7)	2.3672(8)	2.3724(8)	2.3519(5)
Rh1–P4 [Å]				2.4411(7)	2.4483(8)	2.4243(5)
Rh1–B1 [Å]	2.058(1)	2.0796(6)	2.054(3)	2.068(3)	2.109(3)	2.092(2)
Rh1–B2 [Å]	2.005(1)	2.0353(6)	2.015(3)	2.057(3)	2.107(3)	2.082(2)
B1–Rh1–P2 [°]	173.47(4)	163.09(2)	175.51(8)	169.0(1)	161.4(1)	167.43(6)
B2–Rh1–Cl [°]	176.72(4)	176.44(2)	175.63(8)			
B2–Rh1–P4 [°]				172.38(9)	171.98(9)	175.19(7)
P1–Rh1–P3 [°]	166.617(13)	163.446(6)	164.44(3)	158.66(3)	171.85(3)	163.31(2)
B1···B2 [Å]	2.903(2)	2.5678(9)	2.857(4)	2.888(5)	2.574(5)	2.786(3)
B1–Rh1–B2 [°]	91.19(6)	77.21(3)	89.2(1)	88.8(1)	75.3(1)	83.74(8)
τ_{B1}[11] [°]	1.7(1)	83.3(1)	1.8(10)	31(1)	60(1)	53(1)
τ_{B2}[11] [°]	69.5(1)	42.5(1)	61.3(20)	59.8(1)	49(2)	38.7(3)

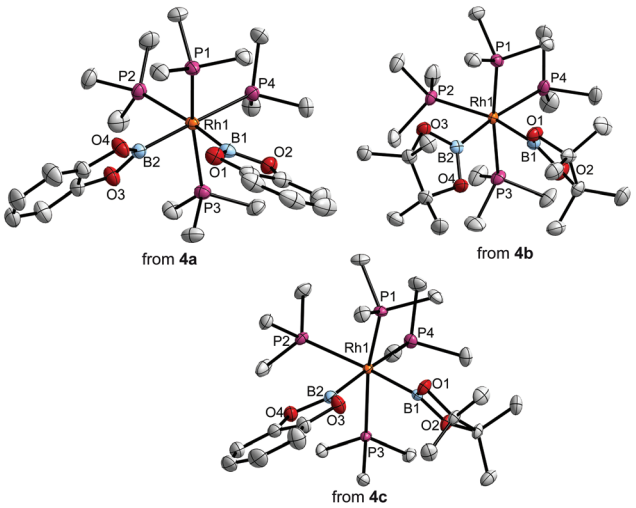

Fig. 4 Molecular structures of the cations in **4a–c** from X-ray diffraction studies on **4a**(PhMe), **4b** and **4c**(THF).[8]

among the complexes **4a–c**, however, do not vary significantly with the individual type of the *trans*-boryl ligand; although the *trans*-Bpin P–Rh distance in **4c** is longer than the *trans*-Bcat P–Rh distance. This is in contrast to the observation of a comparable long P–Rh distance *trans* to the Bpin ligand in **2b** compared to **2a,c**. Again suggesting, that the picture of an virtually exclusive influence of the *trans* ligand on the P–Rh is not comprehensive.

The B···B distance in **4a–c** are in the same range as for **2a–c** with a by >0.2 Å significantly shorter B···B distance for the bis-Bpin complex **4b** than for **4a,c**.

NMR spectroscopic characterisation

The characterisation of **2a–c** by ^{1}H, ^{11}B and ^{31}P NMR spectroscopy shows a set of common characteristic features. The complexes **2a** and **2b** comprising two boryl ligands of the same type at ambient temperature, exhibit in the ^{1}H NMR spectrum at rt only one set of signals for the two structurally distinct boryl moieties (Fig. S1c.1 and 3†[8]). In agreement with that, for the bis-Bpin complex **2b** only one ^{11}B NMR signal is detected at 37.4 ppm ($\Delta w_{1/2}$ = 240 Hz), whereas two distinct signals are observed for the bis-Bcat complex **2a** at 43.2 ppm ($\Delta w_{1/2}$ = 550 Hz) and 47.1 ppm ($\Delta w_{1/2}$ = 620 Hz). The ^{1}H NMR boryl ligand signals of **2a,b**, however, split at lower temperatures, −2 °C for **2a** and −44 °C for **2b**, into individual signals for each boryl ligand (Fig. S1c.1 and 3†[8]).

The ^{31}P NMR data also share many characteristics, for **2a–c** at room temperature two signals are observed, one broadened doublet (due to ^{31}P–^{103}Rh coupling) at −7.2 ± 2.4 ppm for the *trans*-P phosphine ligands and one very broad singlet at lower chemical shifts for the *trans*-B phosphine ligand (**2a** −29.0 ppm ($\Delta w_{1/2}$ = 190 Hz), **2b** −39.2 ppm ($\Delta w_{1/2}$ = 135 Hz) and **2c** −31.2 ppm ($\Delta w_{1/2}$ = 280 Hz)) (Fig. S1c.2, 4 and 12†[8]). At lower temperatures (10 °C for **2a,c** and −44 °C for **2b**) the first signal becomes a doublet of doublets due to the now resolved ^{31}P–^{31}P coupling. The latter signal becomes a more or less well resolved doublet of triplets only at much lower temperatures (*ca.* −60 °C). Whilst the *trans*-P phosphine signals only shifts marginally with temperature (1.5 ppm), the *trans*-B phosphine signals exhibit more distinct shifts towards higher chemical shift upon cooling. However, for the bis-Bpin complex **2b** a significantly wider shift range (−39.2 to −30.2 ppm, 10 ppm), is observed, as for **2a** (−29.0 to −25.5 ppm, 3.5 ppm) and **2c** (−31.2 to −28.0 ppm, 3.2 ppm).

In summary it is concluded that the complexes **2a–c** are dynamic in solution at room temperature, whilst at lower temperature their solution state structures resemble their solid state structures.

Exemplarily the behaviour of **2b** towards excess PMe_3 was studied by ^{31}P NMR spectroscopy (Fig. S1b.16†). It was found that excess PMe_3 leads to a sharpening of the signal of the mutual *trans*-P phosphine ligands at −4.8 ppm but only a minute shift of this signal. Whereas the *trans*-B PMe_3 signal shifts more pronounced from −39 ppm to −59 ppm, whilst the linewidth is not significantly affected; it may be emphasised that no additional signal of free PMe_3 is detected. These data suggest that the *trans*-P PMe_3 ligands do not undergo rapid exchange with free PMe_3, the slight narrowing of these signals rather suggest reduced intramolecular dynamics involving these phosphines in the presence of free PMe_3. In contrast, the *trans*-B ligand undergoes rapid exchange with free PMe_3 leading to a broad, unfeatured singlet with a chemical shift, depending on the amount of PMe_3 present.[8]

An (additional) intramolecular dynamic of predominantly the *trans*-B PMe_3 ligand is suggested by the observation of only one set of boryl ligand signals for **2a,b** at room temperature and it splitting upon cooling, whereas no change is observed for the inherently unsymmetrical complex **2c**.

Also the more pronounced temperature dependence of the *trans*-B phosphine ligand ^{31}P NMR shift in **2b** agrees with this interpretation; the stronger *trans* effect/influence of the Bpin ligand leads to weaker bonding and more labile *trans*-B phosphine ligands.[3b] This fits also to the observation of a five coordinate bis phosphine complex, **3b**, only for the Bpin ligand (*vide infra*).

The NMR data of the five coordinate complex **3b** show little temperature dependence. The ^{31}P NMR spectrum shows independently of the temperature a doublet due to ^{103}Rh–^{31}P coupling, that narrows slightly upon cooling, whereas the ^{1}H NMR signals exhibit some broadening upon cooling. This is in agreement with an absence of dynamic processes for **3b**, in contrast to the highly dynamic behaviour of **2b**. More interesting are the NMR data of the co-crystallised mixture **2b·3b**. This exhibits at room temperature two broadened ^{31}P NMR signals, one singlet around −37 ppm and a doublet around 0 ppm (Fig. 5).

At −90 °C the latter signal has split into a doublet at 4.9 ppm, indicative for **3b** and a doublet of doublets at −5.9 ppm indicative for **2b**. The second signal shifts to −30.2 ppm, as reported for **2b**. It must be concluded that at room temperature **2b** and **3b** are in rapid exchange by dis-

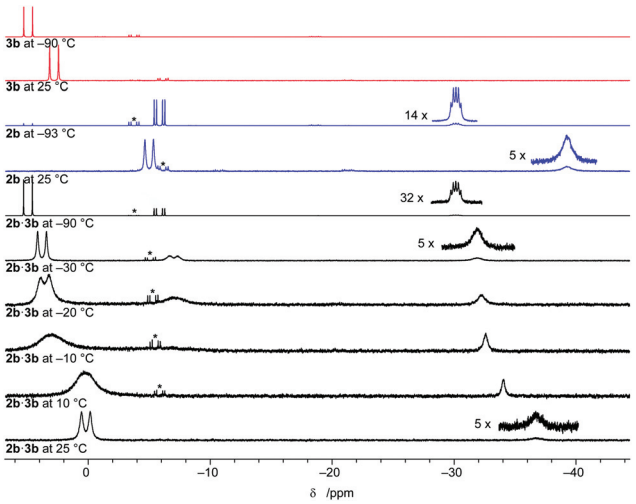

Fig. 5 Variable temperature $^{31}P\{^1H\}$ NMR spectra of **2b·3b**, **2b** and **3b** (162.1 MHz, THF-d_8, * refers to an unassigned impurity).

sociation/association of the *trans*-B PMe_3 ligand. The ratio **2b : 3b** is estimated from the averaged chemical shift in **2b·3b** and the individual chemical shifts for **2b** and **3b** at room temperature to 0.39. This is in good agreement with the ratio **2b : 3b** as suggested by integration of the low temperature $^{31}P\{^1H\}$ and ^1H NMR data of 0.38 and 0.42 and the room temperature ^1H NMR data of 0.43.[8] And is also in agreement with the elemental analysis for this sample.

The ^{31}P NMR spectra of the cationic complexes **4a–c** exhibit the expected two signals for the *trans*-P and *trans*-B PMe_3 ligands as two doublet of triplets for **4a–b**, and a doublet of doublets of doublets and doublet of triplets of doublet for the unsymmetrical **4c**, respectively. However, those complexes exhibit only marginal signal shifts with temperature (<2.5 ppm) but some narrowing upon cooling, suggestive for only little dynamics (Fig. S1d.1, 4 and 6† [8]). The NMR data of **5c** and **6c** are very similar and resemble those of **2c** (Fig. S1d.8 and 10† [8]).

The ^{11}B NMR data of **4a–c**, **5c** and **6c** are however, more insightful. For **4a–c** distinct different ^{11}B NMR shifts are observed for the symmetrical bis-Bcat (**4a**, 44.8 ppm) and bis-Bpin (**4b**, 39.7 ppm) complexes and consequently for the unsymmetrical complex **4c** the two distinct signals are assigned to the Bcat (44.8 ppm) and the Bpin (40.0 ppm) moieties. For the MeCN and MeNC complexes **5c** and **6c** ^{11}B NMR signals at 46.4/46.3 ppm are assigned to the *trans*-P Bcat ligand. To the Bpin ligand the signals at 36.9 ppm for the MeCN complex (**5c**) and at 40.7 ppm for the MeNC complex (**6c**) are assigned. This agrees also with a shift of 38.3 ppm for the Bpin ligand in **2c** *trans* to the chlorido ligand. These data may suggest a minor influence of the ligands *trans* to a boryl ligand on its ^{11}B NMR chemical shift. Moreover, this agrees with the observation of two distinct NMR signals for the distinct Bcat ligands in **2a** of 43.2 ppm (*trans*-Cl) and 47.1 ppm (*trans*-PMe_3).

Conclusions

The rhodium(III) bis-boryl complexes of the type $[(PMe_3)_3Rh(boryl)_2Cl]$ and $[(PMe_3)_3Rh(boryl)_2L]^+$ (boryl = Bpin, Bcat; L = Cl, PMe_3, MeCN, MeNC) share their general structural, NMR spectroscopic and chemical properties. Structurally the complexes comprise distorted octahedrons with two phosphine ligands in the apical positions (*trans*-P phosphine) and the boryl ligands, one phosphine (*trans*-B phosphine) and L in the equatorial plane. The boryl ligands are arranged *cis* to each other, as expected from them being the strongest σ-donating ligands. The individual geometrical properties, however, depend on the nature of the boryl ligands. In the unsymmetrical bis-boryl complexes **2c**, **4c**, **5c** and **6c** the ligand L (L = Cl, PMe_3, MeCN, MeNC) is always *trans* to the boryl ligand with the strongest σ-donor properties and *trans* influence, the Bpin ligand.[3] The bis-Bpin complex $[(PMe_3)_3Rh(Bpin)_2Cl]$ (**2b**) loses easily the *trans*-Bpin phosphine ligand resulting in the five coordinate $[(PMe_3)_2Rh(Bpin)_2Cl]$ (**3b**). According to the heteronuclear NMR data in solution, essentially the similar structures are realised as in the solid state, however, at room temperature all NMR spectra are dynamic to a certain degree. In summary unsymmetrical diboron(4) derivatives have proven useful precursors to otherwise inaccessible unsymmetrical bis-boryl complexes that allow a detailed insight into the coordination properties of boryl ligands.

Experimental

General considerations

PinB–Bcat (**1c**),[7] catB–Bdmab (**1d**),[7] pinB–Bdmab (**1e**),[4a] $[Rh(PMe_3)_3Cl]$,[14a–c] $[Rh(PMe_3)_4Cl]$,[14a–c] $[Rh(PPh_3)_3Cl]$,[14d] PMe_3[14e] and MeNC[14f] were synthesized using literature procedures. All other chemicals were commercially available and were used as received; their purity and identity were checked by appropriate methods. Unless noted otherwise, all solvents were dried using MBraun solvent purification systems, deoxygenated using the freeze–pump–thaw method and stored under purified nitrogen. All manipulations were performed using standard Schlenk techniques under an atmosphere of purified nitrogen or in a nitrogen filled glove box (MBraun). NMR spectra were recorded on Bruker Avance II 300, Avance III HD 300, Avance III 400 or Avance III HD 500 spectrometers. NMR tubes equipped with screw caps (WILMAD) were used and the solvents were dried over potassium/benzophenone and degassed. Chemical shifts (δ) are given in ppm, using the (residual) resonance signal of the solvents for calibration (C_6D_6: ^1H NMR: 7.16 ppm, ^{13}C NMR: 128.06 ppm; THF-d_8: ^1H NMR: 1.72 ppm, ^{13}C NMR: 25.31 ppm).[15] ^{11}B, ^{19}F and ^{31}P NMR chemical shifts are reported relative to pseudo external $BF_3{\cdot}Et_2O$, $CFCl_3$ and 85% phosphoric acid, respectively. ^{13}C, ^{11}B and ^{19}F NMR spectra were recorded employing composite pulse ^1H decoupling unless noted otherwise. If necessary 2D NMR techniques were employed to assign the individual signals (^1H–^1H NOESY (1 s mixing time), ^1H–^1H COSY, ^1H–^{13}C HSQC and

^{1}H–^{13}C HMBC). ^{11}B NMR spectra were processed applying a back linear prediction in order to suppress the broad background signal due to the borosilicate glass in the NMR tube and instrument and a Lorentz type window function (LB = 10 Hz); the spectra were carefully evaluated to ensure that no genuinely broad signals of the sample were suppressed. Melting points were determined in flame sealed capillaries under nitrogen using a Büchi 535 apparatus and are not corrected. Elemental analyses were performed at the Institut für Anorganische und Analytische Chemie of the Technische Universität Carolo-Wilhelmina zu Braunschweig using an Elementar vario MICRO cube instrument. GC/MS data are measured on a Shimadzu GCMS-QP2010SE in positive EI mode (70 eV, 60–700 or 60–1000 *m*/*z*, inject temperature 250 °C, split rate 100 : 1, interface temperature 280 °C, column *ZB-5MS GUARDIAN*, 30 m × 0.25 mm, 0.25 μm thickness, helium carrier gas, temperature program: 3 min 50 °C, heating rate 12 °C min^{-1}, end temperature 300 °C for 8 min or 6 min 40 °C, heating rate 12 °C min^{-1}, end temperature 300 °C for 38 min).

X-ray structure determinations. The single crystals were transferred into inert perfluoroether oil inside a nitrogen-filled glovebox and, outside the glovebox, rapidly mounted on top of a human hair or Hampton loop and placed in the cold nitrogen gas stream on the diffractometer.[16a] The data were either collected on a Rigaku Oxford Diffraction Synergy-S instrument, using mirror-focused CuK$_\alpha$ radiation, a Rigaku Oxford Diffraction Synergy-S instrument, using mirror-focused MoK$_\alpha$ radiation or an Oxford Diffraction Xcalibur EOS instrument using graphite monochromated MoK$_\alpha$ radiation. The reflections were indexed, integrated and absorption corrections were applied as implemented in the CrysAlisPro software package.[16b] The structures were solved employing the program SHELXT and refined anisotropically for all non-hydrogen atoms by full-matrix least squares on all F^2 using SHELXL software.[16c,d] Generally hydrogen atoms were refined employing a riding model; methyl groups were treated as rigid bodies and were allowed to rotate about the E–CH$_3$ bond. During refinement and analysis of the crystallographic data the programs WinGX, Mercury, Diamond, PLATON, OLEX^2 and DSR were used.[16e–k] Unless noted otherwise, the shown ellipsoids represent the 50% probability level and hydrogen atoms are omitted for clarity. Adapted numbering schemes may be used do improve the readability.

[Rh(PMe$_3$)$_3$(Bcat)$_2$Cl] (2a).[1d] [Rh(PMe$_3$)$_3$Cl] (100 mg, 273 μmol, 1 eq.) in toluene (2 mL) and **1a** (75 mg, 315 μmol, 1.15 eq.) in THF (1 mL) were combined at room temperature. Crystallization of a colourless solid started after approx. 2 minutes. After one night at room temperature, the precipitate was separated from the supernatant solution, washed with *n*-pentane (3 × 4 mL) and dried *in vacuo* to give **2b** as a colourless microcrystalline solid (151 mg, 250 μmol, 92%). Single crystals suitable of **2a** for X-ray diffraction analysis were obtained within a few days from a solution in benzene layered with *n*-pentane at rt.

^{1}H NMR (500.3 MHz, THF-d$_8$, rt): δ 1.37 (9 H, d, J = 6.5 Hz, *trans*-B-PMe$_3$), 1.49 (18 H, app. dt, J = 1.0, 3.2 Hz, *trans*-P-PMe$_3$), 6.88 (4 H, br. s, $\Delta w_{1/2}$ = 18.2 Hz, CH$_{cat}$), 7.04–7.09 (4 H, m, CH$_{cat}$). **^{13}C{^{1}H} NMR** (125.8 MHz, THF-d$_8$, rt): δ 18.4 (d, J = 18 Hz, *trans*-B-PMe$_3$), 20.1 (app. t, J = 17 Hz, *trans*-P-PMe$_3$), 111.6 (br. d, J = 60 Hz, $\Delta w_{1/2}$ = 36 Hz, CH$_{cat}$), 121.8 (CH$_{cat}$), 150.6 (C$_{cat}$). **^{11}B{^{1}H} NMR** (160.5 MHz, THF-d$_8$, rt): δ 43.2 (s, $\Delta w_{1/2}$ = 550 Hz), 47.1 (s, $\Delta w_{1/2}$ = 620 Hz). **^{31}P{^{1}H} NMR** (162.1 MHz, THF-d$_8$, rt): δ −29.0 (br. s, $\Delta w_{1/2}$ = 190 Hz, *trans*-B-PMe$_3$), −7.9 (d, J_{P-Rh} = 102 Hz, $\Delta w_{1/2}$ = 22 Hz, *trans*-P-PMe$_3$). **^{1}H NMR** (300.1 MHz, C$_6$D$_6$, rt): δ 1.08 (9 H, d, J = 6.5 Hz, *trans*-B-PMe$_3$), 1.38 (18 H, br. dt, J = 1.0, 3.2 Hz, *trans*-P P(CH$_3$)$_3$), 6.79 (4 H, br. s, $\Delta w_{1/2}$ = 15 Hz, CH$_{cat}$), 7.07 (4 H, br. s, $\Delta w_{1/2}$ = 14 Hz, CH$_{cat}$). **^{11}B{^{1}H} NMR** (96.3 MHz, C$_6$D$_6$, rt): δ 45.1 (s, $\Delta w_{1/2}$ = 858 Hz). **^{31}P{^{1}H} NMR** (121.5 MHz, C$_6$D$_6$, rt): δ −29.9 (br. s, $\Delta w_{1/2}$ = 167 Hz, *trans*-B-PMe$_3$), −8.7 (d, J = 105 Hz, *trans*-P-PMe$_3$). **^{1}H NMR** (400.4 MHz, THF-d$_8$, −103 °C): δ 1.35 (9 H, d, J = 6.7 Hz, *trans*-B-PMe$_3$), 1.45 (18 H, br. s (sh), *trans*-P-PMe$_3$), 6.88–6.93 (2 H, m, CH$_{cat}$), 6.93–6.99 (2 H, m, CH$_{cat}$), 7.14–7.21 (4 H, m, CH$_{cat}$). **^{31}P{^{1}H} NMR** (162.1 MHz, THF-d$_8$, −103 °C): δ −25.6 (dt, $\Delta w_{1/2}$ = 19 Hz, $^{1}J_{P-Rh}$ = 71 Hz, $^{2}J_{P-P}$ = 31 Hz, *trans*-B-PMe$_3$), −6.4 (dd, $\Delta w_{1/2}$ = 3 Hz, $^{1}J_{P-Rh}$ = 100 Hz, $^{2}J_{P-P}$ = 31 Hz, *trans*-P-PMe$_3$). **m.p.**: 188–191 °C (decomp.). **Anal. Calcd** for C$_{21}$H$_{35}$B$_2$ClO$_4$P$_3$Rh C, 41.73; H, 5.84. Found: C, 41.81; H, 5.99.

[Rh(PMe$_3$)$_2$(Bpin)$_2$Cl] (3b). [Rh(PMe$_3$)$_3$Cl] (126 mg, 344 μmol, 1 eq.) and **1b** (100 mg, 393 μmol, 1.15 eq.) were mixed in toluene (5 mL) at room temperature. After 48 h all volatiles were removed *in vacuo* for several hours. The residue was extracted with *n*-pentane (2 × 10 mL) and filtered over Celite. After concentration *in vacuo* (3 mL) the solution was stored at −40 °C to deposit the product as a fine pale yellow to colourless solid. After 16 h, the mother liquor was decanted, the solid washed with cold *n*-pentane (1.5 mL, −40 °C) and dried *in vacuo*. The mother liquor was concentrated to approx. 1.5 mL and stored at −40 °C to give more product. Combined yield: 96 mg, 176 μmol, 51%. Single crystals suitable for X-ray diffraction were obtained upon recrystallization from *n*-pentane at −40 °C.

^{1}H NMR (300.1 MHz, C$_6$D$_6$, rt): δ 1.08 (24 H, s, C(CH$_3$)$_2$), 1.54 (18 H, br. dt, J_{H-P} = 0.8, 3.5 Hz, P(CH$_3$)$_3$). **^{13}C{^{1}H} NMR** (75.5 MHz, C$_6$D$_6$, rt): δ 15.5 (app. dt, J = 1, 15 Hz, P(CH$_3$)$_3$), 25.3 (C(*C*H$_3$)$_2$), 82.0 (*C*(CH$_3$)$_2$). **^{11}B{^{1}H} NMR** (96.3 MHz, C$_6$D$_6$, rt): δ 37.4 (s, $\Delta w_{1/2}$ = 240 Hz). **^{31}P{^{1}H} NMR** (121.5 MHz, C$_6$D$_6$, rt): δ 2.4 (d, J = 116 Hz, P(CH$_3$)$_3$). **^{1}H NMR** (400.4 MHz, THF-d$_8$, rt): δ 1.18 (24 H, s, C(CH$_3$)$_2$), 1.44 (18 H, br. td, J_{H-P} = 1.0, 3.7 Hz, P(CH$_3$)$_3$). **^{31}P{^{1}H} NMR** (162.1 MHz, THF-d$_8$, rt): δ 2.8 (d, J = 119 Hz, P(CH$_3$)$_3$). **^{1}H NMR** (400.4 MHz, THF-d$_8$, −90 °C): δ 1.17 (24 H, s, C(CH$_3$)$_2$), 1.42 (18 H, s, P(CH$_3$)$_3$). **^{31}P{^{1}H} NMR** (162.1 MHz, THF-d$_8$, −90 °C): δ 4.9 (d, J = 117 Hz, P(CH$_3$)$_3$). **m.p.**: 142–158 °C (decomp.). **Anal. Calcd** for C$_{18}$H$_{42}$B$_2$ClO$_4$P$_2$Rh C, 39.71; H, 7.78. Found: C, 39.82; H, 7.94.

[Rh(PMe$_3$)$_3$(Bpin)$_2$Cl]·[Rh(PMe$_3$)$_2$(Bpin)$_2$Cl] (2b·3b). As described above for **3b**, but the exposure to vacuum is kept to approx. 30 min. The crystallization from *n*-pentane at −40 °C results in the co-crystals with the composition [Rh(PMe$_3$)$_3$(Bpin)$_2$Cl]·[Rh(PMe$_3$)$_2$(Bpin)$_2$Cl] (**2b·3b**); note that all single crystals studied from this material had the composition

2b·3b. However, after brief drying *in vacuo* the exact ratio of **2b** to **3b** varies in a range $n(\mathbf{2b}) : n(\mathbf{3b}) = 0.35–1$ depending on the evacuation.

Anal. Calcd for $C_{39}H_{93}B_4Cl_2O_8P_5Rh_2$ (**2b·3b**) C 40.21, H 8.05; for $C_{57}H_{135}B_6Cl_3O_{12}P_7Rh_3$ (**2b**·(**3b**)$_2$) C 40.05, H 7.96; for $C_{75}H_{177}B_8Cl_4O_{16}P_9Rh_4$ (**2b**·(**3b**)$_3$) C 39.97, H 7.92. Found C 40.03, H 8.01. Yield: 138 mg, 61 μmol of (**2b**·(**3b**)$_3$) (245 μmol Rh), 71% with respect to Rh.

[Rh(PMe$_3$)$_3$(Bpin)$_2$Cl] (2b). **3b** (40 mg, 73.5 μmol, 1 eq.) was dissolved in *n*-pentane (3 mL) and PMe_3 (7.6 μL, 5.6 mg, 73.5 μmol, 1 eq.) was added. After approx. 15 min all volatiles are removed *in vacuo* for period of 10 min at rt to give **2b** quantitatively. Single crystals of **2b**(PhMe) suitable for X-ray diffraction were obtained upon crystallization from a solution in PhMe layered with *n*-pentane at −40 °C. Alternatively, the co-crystalized mixture **2b·3b** and to a **3b** equimolar amount of PMe_3 can be used. However, the **2b** obtained is often contaminated with small amounts of **3b**.

^{1}H NMR (400.4 MHz, THF-d$_8$, rt): δ 1.18 (24 H, s, C(CH$_3$)$_2$), 1.26 (9 H, br. d, J_{H-P} = 3.2 Hz, P(CH$_3$)$_3$), 1.52 (18 H, td, J = 0.9, 3.6 Hz, P(CH$_3$)$_3$). **^{11}B{^{1}H} NMR** (96.3 MHz, THF-d$_8$, rt): δ 37.4 (s, $\Delta w_{1/2}$ = 240 Hz). **^{31}P{^{1}H} NMR** (162.1 MHz, THF-d$_8$, rt): δ −39.2 (br. s, $\Delta w_{1/2}$ = 135 Hz, *trans*-B–P(CH$_3$)$_3$), −5.0 (br. d, J_{P-Rh} = 113 Hz, $\Delta w_{1/2}$ = 28 Hz, *trans*-P-P(CH$_3$)$_3$). **^{1}H NMR** (300.1 MHz, C$_6$D$_6$, rt): δ 1.12 (24 H, s, C(CH$_3$)$_2$), 1.17 (9 H, br. d, J_{H-P} = 4.4 Hz, P(CH$_3$)$_3$), 1.50 (18 H, br. t, J = 3.5 Hz, P(CH$_3$)$_3$). **^{13}C{^{1}H} NMR** (75.5 MHz, C$_6$D$_6$, rt): δ 18.4 (d, J_{C-P} = 9.4 Hz, $\Delta w_{1/2}$ = 12 Hz, *trans*-B–P(CH$_3$)$_3$), 19.4 (t, J = 16 Hz, *trans*-P–P(CH$_3$)$_3$), 25.9 (C(*C*H$_3$)$_2$), 81.5 (*C*(CH$_3$)$_2$). **^{11}B{^{1}H} NMR** (96.3 MHz, C$_6$D$_6$, rt): δ 39.2 (s, $\Delta w_{1/2}$ = 275 Hz). **^{31}P{^{1}H} NMR** (121.5 MHz, C$_6$D$_6$, rt): δ −37.9 (s, $\Delta w_{1/2}$ = 62 Hz, *trans*-B–P(CH$_3$)$_3$), −4.8 (d, J_{P-Rh} = 112 Hz, $\Delta w_{1/2}$ = 15 Hz, P(CH$_3$)$_3$).

^{1}H NMR (400.4 MHz, THF-d$_8$, −62 °C): δ 1.15 (12 H, s, C(CH$_3$)$_2$), 1.18 (12 H, s, C(CH$_3$)$_2$), 1.32 (9 H, d, J = 6.1 Hz, P(CH$_3$)$_3$), 1.52 (18 H, br. t, J = 3.2 Hz, P(CH$_3$)$_3$). **^{31}P{^{1}H} NMR** (202.5 MHz, THF-d$_8$, −93 °C): δ −30.2 (dt, $\Delta w_{1/2}$ = 21 Hz, $^1J_{P-Rh}$ = 68 Hz, $^2J_{P-P}$ = 33 Hz, *trans*-B-PMe$_3$), −5.9 (dd, $\Delta w_{1/2}$ = 3 Hz, $^1J_{P-Rh}$ = 112 Hz, $^2J_{P-P}$ = 33 Hz, *trans*-P-PMe$_3$). **m.p.**: 125–133 °C (decomp.). **Anal. Calcd** for $C_{21}H_{51}B_2ClO_4P_3Rh$ C, 40.65; H, 8.28. Found: C, 40.40; H, 8.27.

[Rh(PMe$_3$)$_3$(Bcat)(Bpin)Cl] (2c). *From* [Rh(PMe$_3$)$_3$Cl]: [Rh(PMe$_3$)$_3$Cl] (218 mg, 594 μmol, 1 eq.) and **1c** (168 mg, 683 μmol, 1.15 eq.) were dissolved in toluene (10 mL). Crystallization of a colourless solid started after approx. 5 minutes and was facilitated by storage at −40 °C. After one night, the mother liquor was decanted, concentrated *in vacuo* (5 mL), layered with *n*-pentane (5 mL) and stored at −40 °C. This process was repeated until no further product deposited. The obtained solid were washed with *n*-pentane (2 × 2 mL) and dried *in vacuo* to give **1c** as a colourless microcrystalline solid (330 mg, 539 μmol, 91%).

From [Rh(PMe$_3$)$_4$]Cl: [Rh(PMe$_3$)$_4$]Cl (120 mg, 271 μmol, 1.04 eq.) and **1c** (64 mg, 260 μmol, 1 eq.) were combined in THF (8 mL). The suspension was treated with ultrasound in an ice-cooled water bath for 1.5 h. The, by then, nearly clear mixture was filtered and all volatiles were evaporated. The solid was taken up in THF (1 mL), filtered over a plug of glass wool and stored at −40 °C. After one night, the mother liquor is decanted, the solid washed with *n*-pentane (2 × 2 mL) and dried *in vacuo* to give **2c** as a colourless microcrystalline solid (64 mg, 104 μmol, 40%).

Single crystals of **2c**(THF)$_{1/2}$ suitable for X-ray diffraction were obtained upon crystallization from a solution in THF rt.

^{1}H NMR (400.4 MHz, THF-d$_8$, rt): δ 1.27 (12 H, s, C(CH$_3$)$_2$), 1.41 (9 H, unresolved (overlapping), *trans*-B-PMe$_3$), 1.42 (18 H, app. dt (overlapping), J = 0.8, 3.4 Hz, *trans*-P-PMe$_3$), 6.81–6.88 (2 H, m, CH$_{cat}$), 7.01–7.08 (2 H, m, CH$_{cat}$). **^{13}C{^{1}H} NMR** (75.5 MHz, THF-d$_8$, rt): δ 18.1–18.8 (br. m, *trans*-B-PMe$_3$), 19.8–20.6 (br. m, *trans*-P-PMe$_3$), 25.9 (C(*C*H$_3$)$_2$), 82.5 (*C*(CH$_3$)$_2$), 111.5 (CH$_{cat}$), 121.5 (CH$_{cat}$), 150.8 (C$_{cat}$). **^{11}B{^{1}H} NMR** (96.3 MHz, THF-d$_8$, rt): δ 38.3 (s, $\Delta w_{1/2}$ = 540 Hz), 46.7 (s, $\Delta w_{1/2}$ = 710 Hz). **^{31}P{^{1}H} NMR** (162.1 MHz, THF-d$_8$, rt): δ −31.2 (br. s, $\Delta w_{1/2}$ = 280 Hz, *trans*-B-PMe$_3$), −9.3 (br. d, J_{P-Rh} = 104 Hz, $\Delta w_{1/2}$ = 84 Hz, *trans*-P-PMe$_3$). **^{1}H NMR** (300.1 MHz, C$_6$D$_6$, rt): δ 1.15 (12 H, s, C(CH$_3$)$_2$), 1.20 (9 H, br. d, J = 6.4 Hz, *trans*-B-PMe$_3$), 1.37 (18 H, br. t, J = 3.4 Hz, *trans*-P-PMe$_3$), 6.81–6.88 (2 H, m, CH$_{cat}$), 7.16–7.22 (overlapping with solvent signal, 2 H, m, CH$_{cat}$). **^{11}B{^{1}H} NMR** (96.3 MHz, C$_6$D$_6$, rt): δ 37.7 (s, $\Delta w_{1/2}$ = 370 Hz), 46.7 (s, $\Delta w_{1/2}$ = 399 Hz). **^{31}P{^{1}H} NMR** (121.5 MHz, C$_6$D$_6$, rt): δ −30.8 (br. s, $\Delta w_{1/2}$ = 250 Hz, *trans*-B-PMe$_3$), −9.0 (br. d, J = 111 Hz, *trans*-P-PMe$_3$). **^{1}H NMR** (400.4 MHz, THF-d$_8$, −50 °C): δ 1.27 (12 H, s, C(CH$_3$)$_2$), 1.38 (18 H, t, J = 3.4 Hz, *trans*-P-PMe$_3$), 1.40 (9 H, d, J = 6.5 Hz, *trans*-B-PMe$_3$), 6.85–6.91 (2 H, m, CH$_{cat}$), 7.06–7.12 (2 H, m, CH$_{cat}$). **^{31}P{^{1}H} NMR** (162.1 MHz, THF-d$_8$, −90 °C): δ −28.0 (dt, J_{P-P} = 36 Hz, J_{P-Rh} = 73 Hz, *trans*-B-PMe$_3$), −7.9 (dd, J_{P-P} = 36 Hz, J_{P-Rh} = 105 Hz, *trans*-P-PMe$_3$). **m.p.**: 189–193 °C (decomp.). **Anal. Calcd** for $C_{21}H_{43}B_2ClO_4P_3Rh$ C, 41.18; H, 7.08. Found: C, 41.35; H, 7.07.

[(PMe$_3$)$_4$Rh(Bcat)$_2$][BArF] (4a). Solutions of **2a** (50 mg, 83 μmol, 1 eq.) in THF (1 mL) and Na[BArF] (74 mg, 83 μmol, 1 eq.) in Toluene (1 mL) were mixed at room temperature. PMe_3 (6.9 mg, 9.4 μL, 91 μmol, 1.1 eq.) was added after 5 min and the turbid solution was filtered over Celite. The filtrate was layered with *n*-pentane (4 mL). A microcrystalline material was obtained after 16 h at −40 °C. The mother liquor was decanted, the solid washed with *n*-pentane (2 × 2 mL) and dried *in vacuo*. The obtained solid was dissolved in THF (1.5 mL), layered with *n*-pentane (4 mL) and stored at −40 °C to give a microcrystalline solid. The mother liquor is decanted, the solid washed with *n*-pentane and dried *in vacuo* to give **4a** as a colourless solid (77 mg, 51 μmol, 61%). Single crystals of **4a** (PhMe) suitable for X-ray diffraction were obtained upon crystallization from a solution in PhMe at −40 °C.

^{1}H NMR (500 MHz, THF-d$_8$, rt): δ 1.53 (18 H, app. t, J = 3.4 Hz, PMe$_3$), 1.57–1.60 (18 H, m, PMe$_3$), 7.03–7.05 (4 H, m, 3,4-CH$_{cat}$), 7.23–7.25 (4 H, m, 2,5-CH$_{cat}$), 7.57 (4 H, br. s, $\Delta w_{1/2}$ = 5 Hz, *p*-CH$_{BArF}$), 7.76–7.79 (8 H, m, *o*-CH$_{BArF}$). **^{13}C{^{1}H} NMR** (125.8 MHz, THF-d$_8$, rt): δ 21.4–21.6 (m, PMe$_3$), 22.7 (tt, J_{C-P} = 4, 17 Hz, PMe$_3$), 112.3 (2,5-CH$_{cat}$), 118.2 (sept., J_{C-F} = 3 Hz, *p*-CH$_{BArF}$), 123.2 (3,4-CH$_{cat}$), 125.5 (q, J_{C-F} = 272 Hz, *C*F$_3$), 129.9 (qq, J_{C-F} = 3, 31 Hz, *m*-*C*(CF$_3$)$_{BArF}$), 135.6 (*o*-CH$_{BArF}$), 149.6 (1,6-

C_{cat}), 162.8 (q, J_{C-B} = 50 Hz, *ipso*-C_{BArF}). **$^{11}B\{^1H\}$ NMR** (160.5 MHz, THF-d_8, rt): δ −6.0 (s, $\Delta w_{1/2}$ = 2 Hz, $B(C_8H_3F_6)_4$), 44.8 (br. s, $\Delta w_{1/2}$ = 380 Hz). **$^{19}F\{^1H\}$ NMR** (282.5 MHz, THF-d_8, rt): δ −62.5 (s, BArF). **$^{31}P\{^1H\}$ NMR** (202.5 MHz, THF-d_8, rt): δ −33.6 (br. s, $\Delta w_{1/2}$ = 185 Hz, *trans*-B-PMe_3), −14.0 (dt, J_{P-P} = 28 Hz, J_{P-Rh} = 94 Hz, *trans*-P-PMe_3). **^1H NMR** (400.4 MHz, THF-d_8, −76 °C): δ 1.52 (18 H, br. s, $\Delta w_{1/2}$ = 9 Hz, PMe_3), 1.59 (18 H, br. s, $\Delta w_{1/2}$ = 9 Hz, PMe_3), 7.04–7.10 (4 H, m, 3,4-CH_{cat}), 7.29–7.35 (4 H, m, 2,5-CH_{cat}), 7.74 (4 H, s, *p*-CH_{BArF}), 7.88 (8 H, br. s, $\Delta w_{1/2}$ = 10 Hz, *o*-CH_{BArF}). **$^{31}P\{^1H\}$ NMR** (162.1 MHz, THF-d_8, −76 °C): −31.1 (dt, $\Delta w_{1/2}$ = 22 Hz, $^1J_{P-Rh}$ = 68 Hz, $^2J_{P-P}$ = 28 Hz, *trans*-B-PMe_3), −12.6 (dt, $\Delta w_{1/2}$ = 3 Hz, $^1J_{P-Rh}$ = 93 Hz, $^2J_{P-P}$ = 28 Hz, *trans*-P-PMe_3). **m.p.**: decomp. >175 °C. **Anal. Calcd** for $C_{56}H_{56}B_3F_{24}O_4P_4Rh$ C, 44.60; H, 3.74. Found: C, 44.56; H, 4.07.

[$(PMe_3)_4$Rh(Bpin)$_2$][BArF] (4b). [$Rh(PMe_3)_3Cl$] (50 mg, 136 μmol, 1 eq.) and **1b** (40 mg, 158 μmol, 1.16 eq.) were combined in THF (2 mL). After 24 h at rt Na[BArF] (121 mg, 137 μmol, 1 eq.) is added followed by PMe_3 (approx. 3 min) (17 μL, 12 mg, 164 μmol, 1.2 eq.). The turbid solution was filtered over Celite and layered with *n*-pentane (5 mL). After 16 h at −40 °C a colourless solid had deposited. The mother liquor was decanted, the solid washed with *n*-pentane (2 × 2 mL) and dried *in vacuo* to give **4b** (103 mg, 66 μmol, 49%). Single crystals of **4b** suitable for X-ray diffraction were obtained upon crystallization from a solution in THF layered with *n*-pentane at −40 °C.

^1H NMR (300.3 MHz, THF-d_8, rt): δ 1.28 (24 H, s, $OCMe_2$), 1.47 (18 H, br. s, $\Delta w_{1/2}$ = 6.5 Hz, PMe_3), 1.65 (18 H, app. t, J = 3.4 Hz, PMe_3), 7.57 (4 H, br. s, $\Delta w_{1/2}$ = 4.5 Hz, *p*-CH_{BArF}), 7.76–7.80 (8 H, m, *o*-CH_{BArF}). **$^{13}C\{^1H\}$ NMR** (75.5 MHz, THF-d_8, rt): δ 21.7–22.6 (m, PMe_3), 23.3–24.0 (m, PMe_3), 26.6 (OC$(CH_3)_2$), 83.8 (O$C(CH_3)_2$), 118.2 (sept., J_{C-F} = 4 Hz, *p*-CH_{BArF}), 125.7 (q, J_{C-F} = 274 Hz, CF_3), 130.0 (qq, J_{C-F} = 3, 31 Hz, *m*-$C(CF_3)_{BArF}$), 135.6 (*o*-CH_{BArF}), 149.6 (1,6-C_{cat}), 163 (q, J_{C-B} = 50 Hz, *ipso*-C_{BArF}). **$^{11}B\{^1H\}$ NMR** (96.3 MHz, THF-d_8, rt): δ −6.0 (s, $\Delta w_{1/2}$ = 2 Hz, $B(C_8H_3F_6)_4$), 39.7 (br. s, $\Delta w_{1/2}$ = 300 Hz). **$^{19}F\{^1H\}$ NMR** (282.5 MHz, THF-d_8, rt): δ −62.4 (s, BArF). **$^{31}P\{^1H\}$ NMR** (121.5 MHz, THF-d_8, rt): δ −36.7 (br. s, $\Delta w_{1/2}$ = 140 Hz, *trans*-B-PMe_3), −14.0 (dt, J_{P-P} = 23 Hz, J_{P-Rh} = 104 Hz, *trans*-P-PMe_3).**^1H NMR** (400 MHz, THF-d_8, −70 °C): δ 1.26 (24 H, s, $OCMe_2$), 1.48 (18 H, app. t, J = 2.9 Hz, PMe_3), 1.65 (18 H, app. t, J = 3.2 Hz, PMe_3), 7.70 (4 H, br. s, $\Delta w_{1/2}$ = 4.5 Hz, *p*-CH_{BArF}), 7.78 (8 H, br. s, *o*-CH_{BArF}). **$^{31}P\{^1H\}$ NMR** (162.1 MHz, THF-d_8, −70 °C): −34.9 (dt, $\Delta w_{1/2}$ = 35 Hz, $^1J_{P-Rh}$ = 64 Hz, $^2J_{P-P}$ = 30 Hz, *trans*-B-PMe_3), −13.9 (dt, $\Delta w_{1/2}$ = 4 Hz, $^1J_{P-Rh}$ = 101 Hz, $^2J_{P-P}$ = 30 Hz, *trans*-P-PMe_3). **m.p.**: decomp. >169 °C. **Anal. Calcd** for $C_{56}H_{72}B_3F_{24}O_4P_4Rh$ C, 44.12; H, 4.76. Found: C, 44.05; H, 4.79.

[$(PMe_3)_4$Rh(Bcat)(Bpin)][BArF] (4c). **2c** (50 mg, 82 μmol, 1 eq.) and Na[BArF] (73 mg, 82 μmol, 1 eq.) were combined in THF (2 mL). PMe_3 (6.8 mg, 9.3 μL, 90 μmol, 1.1 eq.) was added after 5 min. The turbid mixture was filtered through a plug of Celite, the filtrate layered with *n*-pentane (4 mL) and stored at −40 °C. After 16 h crystalline material had deposited and the mother liquor was decanted, the solid washed with *n*-pentane (2 × 2 mL) and dried *in vacuo* to give **4c** as a colourless microcrystalline solid (71 mg, 47 mmol, 57%). Single crystals of **4c** (THF) suitable for X-ray diffraction were obtained upon crystallization from a solution in THF layered with *n*-pentane at −40 °C.

^1H NMR (400.4 MHz, THF-d_8, rt): δ 1.33 (12 H, s, OC$(CH_3)_2$), 1.52 (9 H, overlapping, *trans*-B-PMe_3), 1.55 (9 H, d, J_{H-P} = 6.0 Hz, *trans*-B-PMe_3), 1.59 (18 H, t, J_{H-P} = 3.1 Hz, *trans*-P-PMe_3), 6.97–7.01 (2 H, m, CH_{cat}), 7.13–7.18 (2 H, m, CH_{cat}), 7.56 (4 H, br. s, $\Delta w_{1/2}$ = 4.6 Hz, *p*-CH_{BArF}), 7.76–7.80 (8 H, m, *o*-CH_{BArF}). **$^{11}B\{^1H\}$ NMR** (96 MHz, THF-d_8, rt): δ −6.0 (s, $\Delta w_{1/2}$ = 10 Hz, $B(C_8H_3F_6)_4$), 40.0 (br. s, $\Delta w_{1/2}$ = 450 Hz), 44.8 (br. s, $\Delta w_{1/2}$ = 450 Hz). **$^{19}F\{^1H\}$ NMR** (282.5 MHz, THF-d_8, rt): δ −62.4 (s, BArF). **$^{31}P\{^1H\}$ NMR** (162.1 MHz, THF-d_8, rt): δ −36.7 (br. s, $\Delta w_{1/2}$ = 205 Hz, *trans*-B-PMe_3), −35.1 (br. s, $\Delta w_{1/2}$ = 215 Hz, *trans*-B-PMe_3), −14.4 (dt, J_{P-P} = 25 Hz, J_{Rh-P} = 98 Hz, *trans*-P-PMe_3). **^1H NMR** (400.4 MHz, THF-d_8, −50 °C): δ 1.30 (12 H, s, OC$(CH_3)_2$), 1.52 (9 H, d, J_{H-P} = 6.3 Hz, *trans*-B-PMe_3), 1.56 (9 H, d, J_{H-P} = 6.5 Hz, *trans*-B-PMe_3), 1.59 (18 H, app. t, J_{H-P} = 3.0 Hz, *trans*-P-PMe_3), 6.98–7.02 (2 H, m, 3,4-CH_{cat}), 7.18–7.23 (2 H, m, 2,5-CH_{cat}), 7.68 (4 H, br. s, $\Delta w_{1/2}$ = 4.5 Hz, *p*-CH_{BArF}), 7.83–7.89 (8 H, m, *o*-CH_{BArF}).

$^{13}C\{^1H\}$ NMR (100.7 MHz, THF-d_8, −50 °C): δ 20.5 (d, J_{C-P} = 20 Hz, *trans*-B-PMe_3), 22.0 (d, J_{C-P} = 19 Hz, *trans*-B-PMe_3), 22.5 (tt, J_{C-P} = 4, 18 Hz, *trans*-P-PMe_3), 26.3 (OC$(CH_3)_2$), 83.80/83.83 (overlapping, O$C(CH_3)_2$), 112.0 (3,4-CH_{cat}), 118.4 (br. s., $\Delta w_{1/2}$ = 13 Hz, *p*-CH_{BArF}), 122.8 (2,5-CH_{cat}), 125.4 (q, J_{C-F} = 273 Hz, CF_3), 129.9 (q, $\Delta w_{1/2}$ = 10 Hz, J_{C-F} = 31 Hz, *m*-$C(CF_3)_{BArF}$), 135.4 (*o*-CH_{BArF}), 149.6 (1,6-C_{cat}), 162.9 (q, J_{C-B} = 50 Hz, *ipso*-C_{BArF}). **$^{11}B\{^1H\}$ NMR** (128.5 MHz, THF-d_8, −50 °C): δ −6.5 (s, BArF), no boryl signal observed. **$^{19}F\{^1H\}$ NMR** (376.7 MHz, THF-d_8, −50 °C): δ −62.9 (s, BArF). **$^{31}P\{^1H\}$ NMR** (202.5 MHz, THF-d_8, −50 °C): −34.7 (br., $\Delta w_{1/2}$ = 35 Hz, $^1J_{P-Rh}$ = 59 Hz, $^2J_{P-B(-33.1\ ppm)}$ = 31 Hz, $^2J_{P-P(-12.9\ ppm)}$ = 33 Hz, *trans*-B-PMe_3), −33.1 (br. dtd, $\Delta w_{1/2}$ = 20 Hz, $^1J_{P-Rh}$ = 67 Hz, $^2J_{P-B(-34.7\ ppm)}$ = 31 Hz, $^2J_{P-P(-12.9\ ppm)}$ = 24 Hz, *trans*-B-PMe_3), −12.9 (ddd, $\Delta w_{1/2}$ = 5 Hz, $^1J_{P-Rh}$ = 97 Hz, $^2J_{P-P(-34.7\ ppm)}$ = 33 Hz, $^2J_{P-P(-33.1\ ppm)}$ = 24 Hz, *trans*-P-PMe_3). **m.p.**: decomp. >169 °C. **Anal. Calcd** for $C_{56}H_{64}B_3F_{24}O_4P_4Rh$ (**4c**), 44.36; H, 4.25; for $C_{60}H_{72}B_3F_{24}O_5P_4Rh$ (**4c**·THF), 45.37; H, 4.57. Found: C, 45.54; H, 5.12. The presence of one equivalent of co-crystallised THF is in agreement with the crystal structure being (**4c**·THF).

[Rh$(PMe_3)_3$(NCMe)(Bcat)(Bpin)][BArF] (5c). **2c** (42 mg, 69 μmol, 1 eq.) and NaBArF (61 mg, 69 μmol, 1 eq.) were dissolved in a mixture of toluene (2 mL) and MeCN (20 μL, 0.38 mmol, 5.5 eq.). After 5 min at rt the turbid mixture was filtered through a plug of Celite. After a few minutes, precipitation of a colourless solid started which is promoted by layering the mixture with *n*-pentane (4 mL) and storage at −40 °C. After five days the mother liquor was decanted, the solid is washed with *n*-pentane (2 × 2 mL) and dried *in vacuo* to give [Rh$(PMe_3)_3$(NCMe)(Bcat)(Bpin)][BArF] (**5c**) as a microcrystalline solid (69 mg, 47 mmol, 68%). Single crystals of **5c** suitable for X-ray diffraction were obtained from the reaction mixture in PhMe at rt.

^1H NMR (500.3 MHz, THF-d_8, rt): δ 1.32 (12 H, s, C$(CH_3)_2$), 1.44 (18 H, app. t, J = 3.6 Hz, *trans*-P-PMe_3), 1.48 (9 H, d, J_{H-P} =

6.5 Hz, *trans*-B-PMe_3), 2.40 (3 H, br. s, CH_3CN), 6.96–7.00 (2 H, m, CH_{cat}), 7.10–7.15 (2 H, m, CH_{cat}), 7.57 (4 H, s, *p*-CH_{BArF}), 7.76–7.80 (8 H, m, *o*-CH_{BArF}). **$^{13}C\{^1H\}$ NMR** (125.8 MHz, THF-d_8, rt): δ 1.47 (CH_3CN), 18.2 (dt, J = 1, 20 Hz, *trans*-B-PMe_3), 19.6 (tdd, J = 1, 4, 17 MHz, *trans*-P-PMe_3), 25.8 ($C(CH_3)_2$), 83.7 ($C(CH_3)_2$), 112.1 (CH_{cat}), 118.2 (sept., J_{C-F} = 4 Hz, *p*-CH_{BArF}), 122.6 (CH_{cat}), 125.5 (q, J_{C-F} = 272 Hz, CF_3), 130.0 (qq, J_{C-F} = 3, 32 Hz, *m*-$C(CF_3)$), 135.6 (*o*-CH_{BArF}), 150.0 (C_{cat}), 162.8 (q, J_{C-B} = 50 Hz, *ipso*-C_{BArF}). The quaternary C of the MeCN ligand was not detected. **$^{11}B\{^1H\}$ NMR** (160.5 MHz, THF-d_8, rt): δ −6.0 (s, $\Delta w_{1/2}$ = 11 Hz, $B(C_8H_3F_6)_4$), 36.9 (br. s, $\Delta w_{1/2}$ = 318 Hz), 46.4 (br. s, $\Delta w_{1/2}$ = 288 Hz). **$^{19}F\{^1H\}$ NMR** (282.5 MHz, THF-d_8, rt): δ −62.4 (s, $B(C_8H_3F_6)_4$). **$^{31}P\{^1H\}$ NMR** (202.5 MHz, THF-d_8, rt): δ −31.0 (br. s, $\Delta w_{1/2}$ = 192 Hz, *trans*-B-PMe_3), −10.8 (dd, J_{P-P} = 33 Hz, J_{Rh-P} = 105 Hz, *trans*-P–$P(CH_3)_3$). **^1H NMR** (400 MHz, THF-d_8, −80 °C): δ 1.29 (12 H, s, $C(CH_3)_2$), 1.42 (18 H, s, *trans*-P-PMe_3), 1.49 (9 H, d, J_{H-P} = 6.9 Hz, *trans*-B-PMe_3), 2.52 (3 H, s, CH_3CN), 6.99–7.04 (2 H, m, CH_{cat}), 7.15–7.22 (2 H, br. m, CH_{cat}), 7.78 (4 H, s, *p*-CH_{BArF}), 7.91 (8 H, br. s, *o*-CH_{BArF}). **$^{31}P\{^1H\}$ NMR** (162.1 MHz, THF-d_8, −80 °C): δ −29.8 (dt, $\Delta w_{1/2}$ = 21 Hz, J_{P-P} = 34 Hz, J_{Rh-P} = 74 Hz, *trans*-B-PMe_3), −10.1 (dd, $\Delta w_{1/2}$ = 5 Hz, J_{P-P} = 34 Hz, J_{Rh-P} = 104 Hz, *trans*-P-PMe_3). **m.p.**: >158 °C (decomp.). **Anal. Calcd** for $C_{55}H_{58}B_3F_{24}NO_4P_3Rh$ C, 44.60; H, 3.95; N, 0.95. Found: C, 44.17; H, 4.24; N, 1.29.

$[Rh(PMe_3)_3(CNMe)(Bcat)(Bpin)][BArF]$ (6c). **5c** (50 mg, 34 μmol, 1 eq.) was dissolved in THF (2 mL) and MeNC (10 μL, 168 mmol, 5 eq.) was added. The mixture was layered with *n*-pentane (4 mL) and stored at −40 °C. After 16 h a crystalline material had deposited, the mother liquor was decanted, the crystalline residue washed with *n*-pentane (2 × 2 mL) and dried under reduced pressure. The washing solution was added to the mother liquor, from which additional crystalline material deposited within few days at −40 °C. The solids are dried *in vacuo* to give $[Rh(PMe_3)_3(CNMe)(Bcat)(Bpin)][BArF]$ (**6c**) as a crystalline material (34 mg, 23 μmol, 68%). Single crystals of **6c** suitable for X-ray diffraction were obtained from THF solution layered with *n*-pentane at −40 °C.

^1H NMR (500.3 MHz, THF-d_8, rt): δ 1.34 (12 H, s, $C(CH_3)_2$), 1.48 (18 H, app. t, J = 3.7 Hz, *trans*-P-PMe_3), 1.52 (9 H, d, J_{H-P} = 6.8 Hz, *trans*-B-PMe_3), 3.57 (3 H, CH_3NC, overlapping with solvent signal), 6.97–7.01 (2 H, m, CH_{cat}), 7.11–7.15 (2 H, m, CH_{cat}), 7.57 (4 H, s, *p*-CH_{BArF}), 7.76–7.80 (8 H, m, *o*-CH_{BArF}). **$^{13}C\{^1H\}$ NMR** (125.8 MHz, THF-d_8, rt): δ 19.9 (dt, J = 2, 22 Hz, *trans*-B-PMe_3), 21.3 (tdd, J = 1, 4, 18 MHz, *trans*-P-PMe_3), 25.9 ($C(CH_3)_2$), 29.0 (br. s, $\Delta w_{1/2}$ = 13 Hz, CH_3CN), 83.5 ($C(CH_3)_2$), 112.1 (CH_{cat}), 118.2 (sept., J_{C-F} = 4 Hz, *p*-CH_{BArF}), 122.7 (CH_{cat}), 125.5 (q, J_{C-F} = 272 Hz, CF_3), 130.0 (qq, J_{C-F} = 3, 32 Hz, *m*-$C(CF_3)$), 135.6 (*o*-CH_{BArF}), 145.3 (br., CH_3NC), 150.1 (two signals, C_{cat}), 162.8 (q, J_{C-B} = 50 Hz, *ipso*-C_{BArF}). **$^{11}B\{^1H\}$ NMR** (160.5 MHz, THF-d_8, rt): δ −6.0 (s, $\Delta w_{1/2}$ = 3 Hz, $B(C_8H_3F_6)_4$), 40.7 (br. s, $\Delta w_{1/2}$ = 280 Hz), 46.3 (br. s, $\Delta w_{1/2}$ = 390 Hz). **$^{19}F\{^1H\}$ NMR** (282.5 MHz, THF-d_8, rt): δ −62.4 (s, $B(C_8H_3F_6)_4$). **$^{31}P\{^1H\}$ NMR** (202.5 MHz, THF-d_8, rt): δ −31.5 (br. s, $\Delta w_{1/2}$ = 170 Hz, *trans*-B-PMe_3), −11.5 (dd, J_{P-P} = 32 Hz, J_{Rh-P} = 99 Hz, *trans*-P-$P(CH_3)_3$). **^1H NMR** (400 MHz, THF-d_8, −80 °C): δ 1.31 (12 H, s, $C(CH_3)_2$), 1.46 (18 H, s, *trans*-P-PMe_3), 1.53 (9 H, d, J_{H-P} = 7.1 Hz, *trans*-B-PMe_3), 3.64 (3 H, s, CH_3CN), 6.98–7.05 (2 H, m, CH_{cat}), 7.16–7.22 (2 H, m, CH_{cat}), 7.77 (4 H, s, *p*-CH_{BArF}), 7.89 (8 H, br. s, *o*-CH_{BArF}).**$^{31}P\{^1H\}$ NMR** (162.1 MHz, THF-d_8, −80 °C): δ −30.3 (dt, J_{P-P} = 33 Hz, J_{Rh-P} = 73 Hz, $\Delta w_{1/2}$ = 19 Hz, *trans*-B-PMe_3), −11.0 (dd, J_{P-P} = 33 Hz, J_{Rh-P} = 97 Hz, $\Delta w_{1/2}$ = 5 Hz, *trans*-P-PMe_3). **Anal. Calcd** for $C_{55}H_{58}B_3F_{24}NO_4P_3Rh$ C, 44.60; H, 3.95; N, 0.95. Found: C, 44.63; H, 3.59; N, 1.24. **m.p.**: >148 °C (decomp.).

Conflicts of interest

There are no conflicts to declare.

Acknowledgements

C. K. and W. D. gratefully acknowledge support by a Research Grant (KL 2243/5-1) of the Deutsche Forschungsgemeinschaft (DFG). The authors thank AllyChem Co. Ltd for a generous gift of diboron reagents.

Notes and references

1 (*a*) J. F. Hartwig, K. S. Cook, M. Hapke, C. D. Incarvito, Y. Fan, C. E. Webster and M. B. Hall, *J. Am. Chem. Soc.*, 2005, **127**, 2538–2552; (*b*) M. V. Câmpian, J. L. Harris, N. Jasim, R. N. Perutz, T. B. Marder and A. C. Whitwood, *Organometallics*, 2006, **25**, 5093–5104; (*c*) C. Dai, G. Stringer, T. B. Marder, A. J. Scott, W. Clegg and N. C. Norman, *Inorg. Chem.*, 1997, **36**, 272–273; (*d*) W. Clegg, F. J. Lawlor, T. B. Marder, P. Nguyen, N. C. Norman, A. G. Orpen, M. J. Quayle, C. R. Rice, E. G. Robins, A. J. Scott, F. E. S. Souza, G. Stringer and G. R. Whittell, *J. Chem. Soc., Dalton Trans.*, 1998, 301–310; (*e*) R. T. Baker, J. C. Calabrese, S. A. Westcott, P. Nguyen and T. B. Marder, *J. Am. Chem. Soc.*, 1993, **115**, 4367–4368; (*f*) G. J. Irvine, M. J. G. Lesley, T. B. Marder, N. C. Norman, C. R. Rice, E. G. Robins, W. R. Roper, G. R. Whittell and L. J. Wright, *Chem. Rev.*, 1998, **98**, 2685–2722.

2 (*a*) E. C. Neeve, S. J. Geier, I. A. I. Mkhalid, S. A. Westcott and T. B. Marder, *Chem. Rev.*, 2016, **116**, 9091–9916; (*b*) T. Ishiyama and N. Miyaura, *Chem. Rec.*, 2004, **3**, 271–280.

3 (*a*) J. Zhu, Z. Lin and T. B. Marder, *Inorg. Chem.*, 2005, **44**, 9384–9390; (*b*) H. Braunschweig, P. Brenner, A. Müller, K. Radacki, D. Rais and K. Uttinger, *Chem. – Eur. J.*, 2007, **13**, 7171–7176.

4 (*a*) C. Borner and C. Kleeberg, *Eur. J. Inorg. Chem.*, 2014, 2486–2489; (*b*) W. Drescher, C. Borner, D. J. Tindall and C. Kleeberg, *RSC Adv.*, 2019, **9**, 3900–3911.

5 (*a*) W. Drescher, D. Schmitt-Monreal, C. R. Jacob and C. Kleeberg, *Organometallics*, 2020, **39**, 538–543; (*b*) C. Dai, G. Stringer, J. F. Corrigan, N. J. Taylor, T. B. Marder and N. C. Norman, *J. Organomet. Chem.*, 1996, **513**, 273–275; (*c*) A. S. Batsanov, J. C. Collings and T. B. Marder, 2004,

CCDC number 244650.† (*d*) C. J. Adams, R. A. Baber, A. S. Batsanov, G. Bramham, J. P. H. Charmant, M. F. Haddow, J. A. K. Howard, W. H. Lam, Z. Lin, T. B. Marder, N. C. Norman and A. G. Orpen, *Dalton Trans.*, 2006, 1370–1373.

6 H. Schubert, W. Leis, H. A. Mayer and L. A. Wesemann, *Chem. Commun.*, 2014, **50**, 2738–2740.

7 W. Oschmann, C. Borner and C. Kleeberg, *Dalton Trans.*, 2018, **47**, 5318–5327.

8 See ESI† for further data.

9 To the best of our knowledge there is only one example of an oxidative addition of a tetra amino diborane(4) derivative: G. Wang, L. Xu and P. Li, *J. Am. Chem. Soc.*, 2015, **137**, 8058–8061.

10 Performing the reaction of equimolar amounts of [Rh(PMe_3)$_3$Cl] and **1d** in THF led after 8 d at rt to the deposition of small amount of small pale single crystals. X-ray structure determination suggests that these crystals are [(Me_3P)$_4$Rh H(Cl)][$Bcat_2$](THF).[8] GCMS analysis of the mother liquor indicated also the formation of the symmetrical diborane(4) B_2dmab_2. After shorter reaction times and addition of *n*-pentane only [Rh(PMe_3)$_3$Cl] was obtained. Note that the related species [(Me_3P)$_4$Rh H(Cl)][B(1,2-$O_2C_6Br_4$)$_2$] was reported to be formed upon reaction of [Rh(PMe_3)$_4$]Cl with B_2(1,2-$O_2C_6Br_4$)$_2$. N. C. Norman, A. G. Orpen, M. J. Quayle and E. G. Robins, *Acta Crystallogr., Sect. C: Cryst. Struct. Commun.*, 2000, **56**, 50–52.

11 τBX is defined as the angle included by mean plane of the rhodium atom and the equatorial ligand atoms [Rh1, B1, B2, (P2), Cl1 or P4] and mean plane of the boron atom BX and the three atoms bound to BX [B1, O, O′, Rh1].

12 M. A. Esteruelas, I. Fernández, A. Martínez, M. Oliván, E. Oñate and A. Vélez, *Inorg. Chem.*, 2019, **58**, 4712–4717.

13 (*a*) W. Oschmann, C. Borner and C. Kleeberg, *Dalton Trans.*, 2018, **47**, 5318–5327; (*b*) W. Clegg, M. R. J. Elsegood, F. J. Lawlor, N. C. Norman, N. L. Pickett, E. G. Robins, A. J. Scott, P. Nguyen, N. J. Taylor and T. B. Marder, *Inorg. Chem.*, 1998, **37**, 5289–5293.

14 (*a*) G. Giordano, R. H. Crabtree, R. M. Heintz, D. Forster and D. E. Morris, in *Inorganic Syntheses*, ed. R. J. Angelici, Wiley-Interscience, Hoboken, N.J., 1990, 28, pp. 88–90; (*b*) R. T. Price, R. A. Andersen and E. L. Muetterties, *J. Organomet. Chem.*, 1989, **376**, 407–417; (*c*) R. A. Jones, F. M. Real, G. Wilkinson, A. M. R. Galas, M. B. Hursthouse and K. M. A. Malik, *J. Chem. Soc., Dalton Trans.*, 1980, 511–518; (*d*) P. G. Gassman, D. W. Macomber and S. M. Willging, *J. Am. Chem. Soc.*, 1985, **107**, 2380–2388; (*e*) M. L. Luetkens, A. P. Sattelberger, H. H. Murray, D. J. Basil, J. P. Fackler, R. A. Jones and D. E. Heaton, in *Inorganic Syntheses*, ed. R. J. Angelici, Wiley-Interscience, Hoboken, N.J., 1990, pp. 305–310; (*f*) R. R. Schuster, J. E. Scott and J. Casanova Jr., *Org. Synth.*, 1966, **46**, 75–77.

15 G. R. Fulmer, A. J. M. Miller, N. H. Sherden, H. E. Gottlieb, A. Nudelman, B. M. Stoltz, J. E. Bercaw and K. I. Goldberg, *Organometallics*, 2010, **29**, 2176–2179.

16 (*a*) D. Stalke, *Chem. Soc. Rev.*, 1998, **27**, 171–178; (*b*) *CrysAlisPro*, Agilent Technologies, 2015–2018; (*c*) G. M. Sheldrick, *Acta Crystallogr., Sect. A: Found. Adv.*, 2015, **71**, 3–8; (*d*) G. M. Sheldrick, *Acta Crystallogr., Sect. C: Struct. Chem.*, 2015, **71**, 3–8; (*e*) L. J. Farrugia, *J. Appl. Crystallogr.*, 1999, **32**, 837–838; (*f*) C. F. Macrae, I. Sovago, S. J. Cottrell, P. T. A. Galek, P. McCabe, E. Pidcock, M. Platings, G. P. Shields, J. S. Stevens, M. Towler and P. A. Wood, *J. Appl. Crystallogr.*, 2020, **53**, 226–235; (*g*) H. Putz and K. Brandenburg, *Crystal Impact*, Bonn, Germany, 2018; (*h*) A. L. Spek, *Acta Crystallogr., Sect. C: Struct. Chem.*, 2015, **71**, 9–18; (*i*) A. L. Spek, *Acta Crystallogr., Sect. D: Biol. Crystallogr.*, 2009, **65**, 148–155; (*j*) O. V. Dolomanov, L. J. Bourhis, R. J. Gildea, J. A. K. Howard and H. Puschmann, *J. Appl. Crystallogr.*, 2009, **42**, 339–341; (*k*) D. Kratzert and I. Krossing, *J. Appl. Crystallogr.*, 2018, **51**, 928–934.